

An anomaly in the glass transition width trends of alkali borate glasses at low modifier loadings

A. DeCeanne, A. Potter, K. Richter, D. Starkenburg, B. Perez, T. Munhollon, N. Barnes, E. Troendle, C. Flynn, M. Affatigato, S. Feller*

Center for the Study of Glass, Coe College, Cedar Rapids, Iowa 52402, USA

E. Zanotto & O. Pietl

Federal University of São Carlos, São Carlos, São Paulo, Brazil

Manuscript received 30 January 2017

Revised version received 22 March 2017

Accepted 24 March 2017

The glass transition onset temperature (T_g), the glass transition end temperature (T_e), and the glass transition width (ΔT_g) of alkali borate glasses were determined using differential scanning calorimetry (using the definition $\Delta T_g \equiv T_e - T_g$). An anomaly was found in ΔT_g trends of the lighter alkali modifiers, with that of lithium being the most prominent. From $R=0.03$ to 0.10 , where R is the molar ratio of alkali oxide to boron oxide, ΔT_g values of the lithium family experience a large increase, maximizing at $R=0.05$. Those of the sodium family experience a smaller increase. After $R=0.10$, the trends of all alkali borates follow a similar monotonic decline. An explanation based on thermodynamic modelling of the borate species, as well as viscosity, is proposed.

1. Introduction

Previous studies conducted at Coe College have examined the glass transition width (ΔT_g) among alkali borate glasses. Munhollon *et al.*⁽¹⁾ and Starkenburg *et al.*⁽²⁾ discovered anomalies in the widths of the glass transition of alkali borate glasses at low alkali contents. Masao Kodama has also studied these thermal properties; Kodama's published T_g data exhibit an identical, albeit unmentioned, anomaly.⁽³⁾

The anomaly has been verified, and the dataset widely expanded to more fully cover the compositional range. Onset definitions were used for T_g and T_e .⁽³⁾ ΔT_g is defined as $T_e - T_g$. This study describes the anomaly and provides an explanation based on Shakhmatkin *et al.*'s thermodynamic model of glass structure.⁽⁴⁾ The basis of the Shakhmatkin *et al.*'s approach is that the glass is composed of structural groupings from various associated crystalline stoichiometries. Knowledge of borate crystal structures were taken from Wright *et al.*⁽⁵⁾ The concept of the fictive temperature (the temperature at which the glass structure is frozen in) along with a modified view of constraint theory was also employed in which the chemical groupings used were the superstructural units rather than the short range structures.⁽⁶⁾ We use the superstructural groupings rather than the short

range trigonal and tetrahedral borons proposed by Mauro *et al.*⁽⁷⁾ since there is no difference in the abundances of the short range units between any of the alkali borate series in this range of composition.

2. Experimental procedures

A. Sample preparation

Glass samples were made as follows: (1) 6 g of reagent grade or better alkali carbonates and boric acid obtained from the Sigma-Aldrich company were used as the starting chemicals. The compounds were measured into a platinum crucible and thoroughly mixed for 5 min. The composition is described by R , the molar ratio of alkali oxide to boron oxide. (2) The sample was then heated for fifteen minutes at 1000°C . At that point, (3) weight loss of the sample was determined and compared to a prediction made from stoichiometry. Samples matched predicted weight losses to within 0.1 g. (4) The sample was then returned to the furnace and heated for another 5 min, again at 1000°C . (5) Finally, the melt was quenched between two steel plates, resulting in clear glass which was subsequently stored in a desiccator. Our previous work in making glasses, which has been published extensively, has shown that the water content typically makes up a few hundredths of a percent of the total mass when glasses are made in this manner.

* Corresponding author. Email sfeller@coe.edu
DOI: 10.13036/17533562.58.5.004

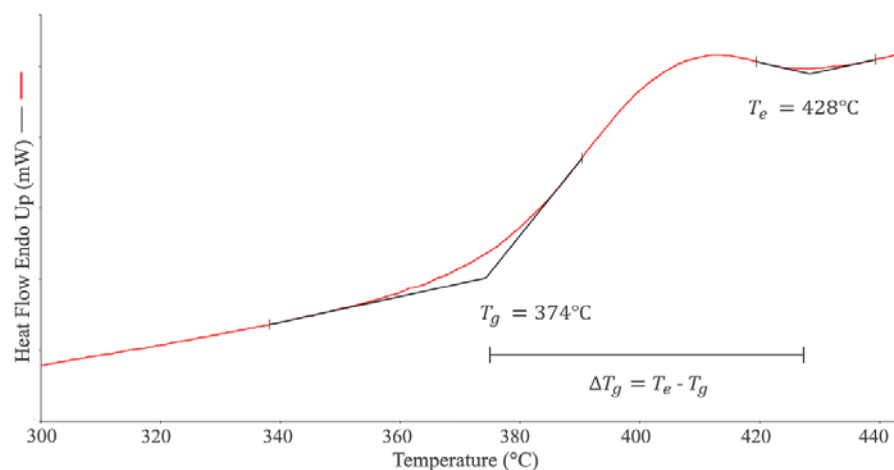


Figure 1. An example DSC trace (potassium borate glass with $R=0.14$, where R is the molar ratio of modifier to glass former) which includes the definitions of T_g and T_e . Here, ΔT_g is simply the disparity in temperature between the two intersection points seen above; in short, $\Delta T_g = T_e - T_g$ [Colour available online]

B. DSC analysis

In order to maintain a uniform thermal treatment between samples, the Perkin-Elmer Diamond differential scanning calorimeter (DSC) was programmed as follows: the sample was (1) held at 50°C for 1 min, (2) heated from 50°C to 550°C at 40°C/min, (3) held at 550°C for 1 min, (4) cooled from 550°C to 50°C at 40°C/min, (5) held at 50°C for one minute, and (6) heated again from 50°C to 550°C at 40°C/min. This process ensures uniform heating and cooling rates for all samples. Previous glass transition temperature measurements from this group have consistently used 40°C/min and for that reason the rate was kept identical for the present work. Measurements at 20°C/min were also performed and were found to have only small variations in the glass transition and its width.

In some cases, however, a lower maximum temperature was used in steps (2)–(4) in order to avoid crystallization; this alteration was not made for the final heating step (step (6)), as samples were not reused after analysis. T_g and T_e were calculated by determining onset points before and after the glass transition – see Figure 1. ΔT_g was calculated by subtracting T_g from T_e . Experimental error in both the T_g and T_e data sets is $\pm 2^\circ\text{C}$, as determined through calibration using indium and zinc, as well as sample-to-sample variation. Experimental error in the ΔT_g data set is $\pm 3^\circ\text{C}$. Samples rapidly quenched (rates greater than 10000°C/s) were tested to see if the quench rate affected the transition width. Little, if any, effect was noted.

C. Penetration viscometry

Penetration viscometry measures the rate of penetration (in m/s) of a cylindrical indenter into a glass piece under isothermal conditions and a known load. Using appropriate relations between the load

and the cylinder diameter, the penetration method is able to determine viscosities in the range 10^7 – 10^{15} Pas with an estimated accuracy of $\log_{10}\eta = \pm 0.1$, via the Slavyanski equation:⁽⁷⁾

$$\eta = m \frac{(1 - \mu^2)P}{2\sqrt{\pi}Rv} \quad (1)$$

where η is the viscosity of the sample (Pas), μ is Poisson's ratio (unitless), P is the applied force (N), R is the radius of the cylinder, m is a constant that dependent on the indenter, and v is the penetration rate (m/s). For a cylindrical indenter:

$$m = \frac{16}{(3\sqrt{\pi})^2} = 2.486 \quad (2)$$

The schematic representation of the penetrometer is shown in Figure 2. Here, the furnace can reach temperatures up to 1000°C; the indenter is made from the nickel–chromium alloy NIMONIC 80A; and a stem composed of ZAS ceramic⁽⁸⁾ connects the indenter to the weight pan. Two thermocouples are used (each

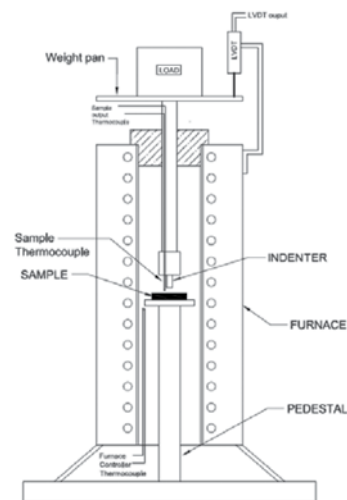


Figure 2. Schematic of the penetration viscometer (named EDos after EDgar and OScar, its creators)

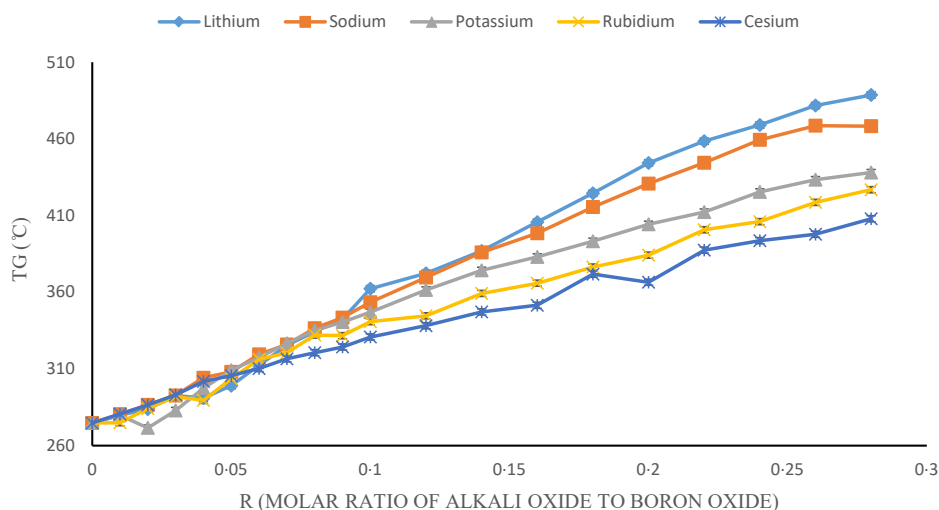


Figure 3. T_g values of alkali borate glasses as a function of R (molar ratio of alkali oxide to boron oxide). Error bars are approximately the size of the data points [Colour available online]

Table 1. T_g values for alkali borate glasses (in °C) as a function of R (molar ratio of alkali oxide to boron oxide). Experimental error in the T_g data set is $\pm 2^\circ\text{C}$

Composition R	X	Lithium T_g (in °C)	Sodium T_g (in °C)	Potassium T_g (in °C)	Rubidium T_g (in °C)	Caesium T_g (in °C)
0	0	275	275	275	275	275
0.01	0.0099	280	280	280	275	281
0.02	0.0196	284	287	272	284	287
0.03	0.0291	293	293	283	292	293
0.04	0.0385	291	304	297	289	302
0.05	0.0476	299	308	309	304	306
0.06	0.0566	312	319	317	316	310
0.07	0.0654	325	326	327	320	317
0.08	0.0741	334	337	335	332	321
0.09	0.0826	342	343	341	332	324
0.1	0.0909	362	353	347	341	331
0.12	0.1071	372	370	362	345	338
0.14	0.1228	387	386	374	359	347
0.16	0.1193	408	398	383	366	351
0.18	0.1525	425	416	393	376	372
0.2	0.1667	444	431	404	384	367
0.22	0.1803	459	444	412	401	387
0.24	0.1935	469	459	425	406	394
0.26	0.2063	482	469	433	419	398
0.28	0.2188	489	468	438	427	408

87% platinum/13% rhodium alloy), one controlling the furnace temperature and the other monitoring the sample surface. The indenter used was 2 mm in diameter and the load varied between 5 and 180 N.

Substituting these values into the above equation, and taking μ to be 0.5,⁽⁹⁾ the following is obtained:

$$\eta = 138.56 \frac{P}{v} \quad (3)$$

Therefore, for calculating viscosity at constant load and temperature, only the penetration rate must be measured. This is determined by recording the displacement, as detected by a linear variable differential transformer (LVDT) as a function of time.

Samples were (1) polished with 600 grit sandpaper. Sample shape is unimportant; however, its surface area must be between 1.5 and 3.2 cm², with thicknesses between 4 and 10 mm. Samples were (2) placed in the instrument with the indenter centered

on the glass, (3) the furnace was stabilized to roughly 10°C below T_g , and (4) the maximum load of 181 N was applied. (5) The furnace temperature was then increased by 15–20°C and stabilized. (6) The load was then decreased by 10–15%. Steps (5) and (6) are repeated until the load applied is only that from the indenter assembly (5 N), where measurable viscosities are on the order of 10⁷ Pas. In general, this process results in between 9 and 12 experimental points per sample.

3. Results

Values for T_g are shown in Table 1 and Figure 3, while those for T_e are shown in Table 2 and Figure 4. T_g values for all modifiers increase similarly until $R=0.10$, where trends begin to diverge while still increasing. T_g values generally trend higher to lower in order of atomic number. T_g and T_e were observed to monotonically

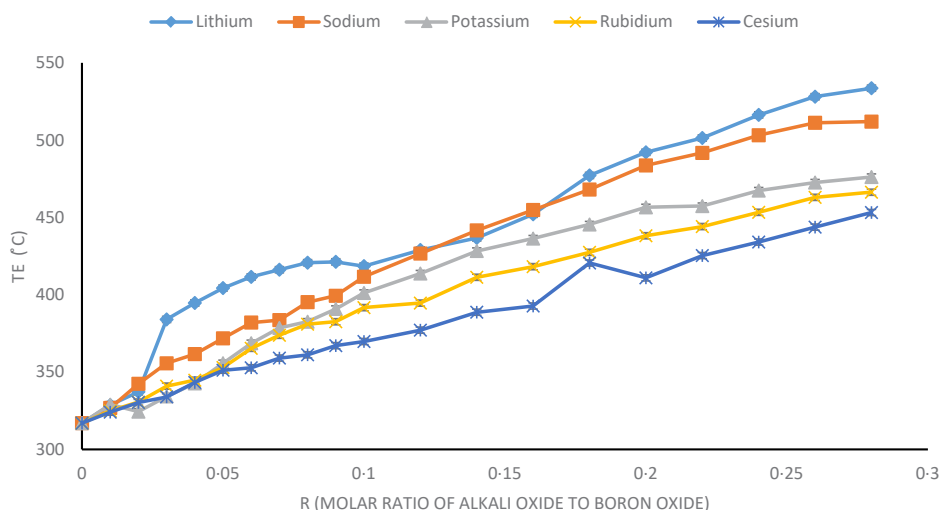


Figure 4. T_g values of alkali borate glasses as a function of R (molar ratio of alkali oxide to boron oxide). Error bars are approximately the size of the data points [Colour available online]

Table 2. T_g values for alkali borate glasses (in °C) as a function of R (molar ratio of alkali oxide to boron oxide). Experimental error in the T_g data set is $\pm 2^\circ\text{C}$

Composition R X	Lithium T_g (in °C)	Sodium T_g (in °C)	Potassium T_g (in °C)	Rubidium T_g (in °C)	Caesium T_g (in °C)
0 0	317	317	317	317	317
0.01 0.0099	329	327	329	325	324
0.02 0.0196	337	342	324	331	330
0.03 0.0291	384	356	334	341	334
0.04 0.0385	395	362	343	345	343
0.05 0.0476	404	372	356	353	351
0.06 0.0566	412	382	369	365	353
0.07 0.0654	416	384	379	374	359
0.08 0.0741	421	395	383	381	361
0.09 0.0826	421	399	391	383	367
0.1 0.0909	419	412	401	392	370
0.12 0.1071	429	427	414	395	377
0.14 0.1228	437	442	428	411	389
0.16 0.1193	452	455	436	418	393
0.18 0.1525	477	468	445	427	421
0.2 0.1667	492	484	457	439	411
0.22 0.1803	501	492	457	444	425
0.24 0.1935	516	503	467	453	434
0.26 0.2063	528	511	473	463	444
0.28 0.2188	534	512	476	466	453

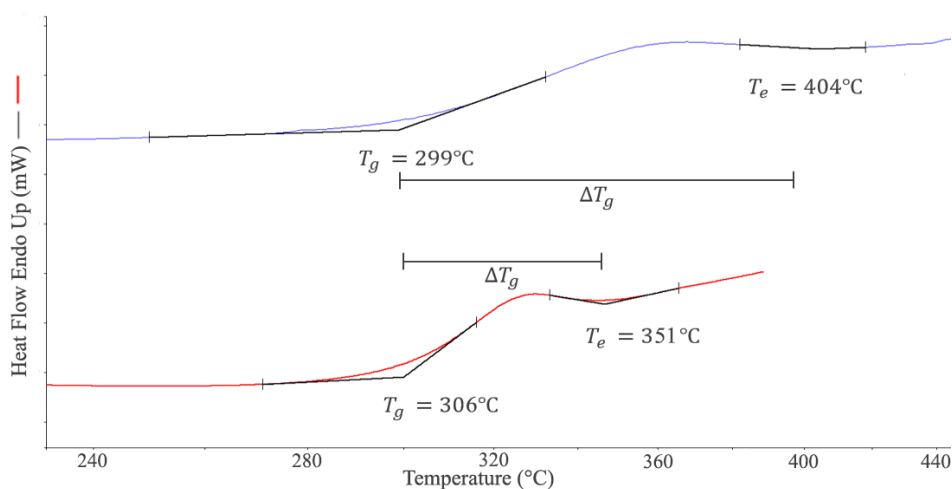


Figure 5. Superimposed DSC traces from $R=0.05$ lithium borate (top) and $R=0.05$ caesium borate (bottom). This comparison shows that the two glasses' transitions begin at similar temperatures but end at widely disparate temperatures [Colour available online]

cally increase, except in the case of lithium borate T_e values; T_e values for the lithium family undergo a rapid increase away from the those of other modifiers beginning at $R=0.03$, and returning to the other alkali trends following $R=0.10$ – see Figure 4. Above $R=0.10$ the lithium curve begins to more closely match those of the other modifiers. The sodium family experiences a smaller increase in the T_e values.

The ΔT_g values are shown in Table 3 and Figure 6. Trends for potassium, rubidium, and caesium families remained relatively constant across composition. Lithium and sodium families experience maximal ΔT_g from $R=0.03$ to 0.10 and then flatten out similarly to the other modifiers.

Figure 7 displays the logarithm of viscosity as a function of inverse temperature for lithium and caesium borate glasses. Uncertainty in the viscosity data is smaller than 0.1 on the log scale, typically 0.05 .

4. Discussion

This study's lithium borate results were compared to those of Kodama *et al.*⁽³⁾ and both data sets were found to display a peak in ΔT_g centred around $R=0.05$. Additionally, trends match between data sets, Figure 8.

Figure 3 shows that T_g values are nearly independent of alkali species within the range $0 \leq R \leq 0.10$. T_e data plotted in Figure 4 indicate a strong dependence on alkali species within the same composition range. T_e values of lighter modifiers are higher than those of the heavier modifiers, resulting in larger ΔT_g values – Figure 5 compares DSC traces of lithium and caesium at $R=0.05$.

In the range of R values following the anomaly from $R=0.10$ to 0.28 , ΔT_g for all alkali modifiers trend similarly, though T_g and T_e values vary in this same range. This is illustrated in Figure 9, where for two glasses both the T_g and T_e of the caesium-modified

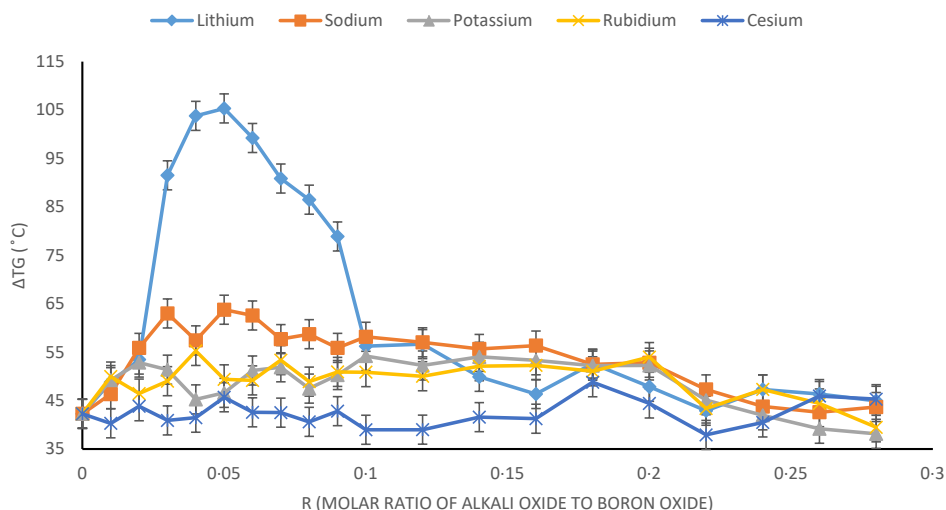


Figure 6. ΔT_g values of alkali borate glasses as a function of R (molar ratio of alkali oxide to boron oxide) [Colour available online]

Table 3. ΔT_g values for alkali borate glasses (in °C) as a function of R (molar ratio of alkali oxide to boron oxide). Experimental error in the ΔT_g data set is $\pm 3^\circ\text{C}$

Composition R	X	Lithium ΔT_g (in °C)	Sodium ΔT_g (in °C)	Potassium ΔT_g (in °C)	Rubidium ΔT_g (in °C)	Caesium ΔT_g (in °C)
0	0	42	42	42	42	42
0.01	0.0099	49	46	49	50	40
0.02	0.0196	53	56	53	46	44
0.03	0.0291	92	63	51	49	41
0.04	0.0385	104	57	45	55	41
0.05	0.0476	105	64	47	49	46
0.06	0.0566	99	63	51	49	43
0.07	0.0654	91	58	52	53	43
0.08	0.0741	87	59	47	49	41
0.09	0.0826	79	56	50	51	43
0.1	0.0909	56	58	54	51	39
0.12	0.1071	57	57	52	50	39
0.14	0.1228	50	56	54	52	42
0.16	0.1193	46	56	53	52	41
0.18	0.1525	53	52	52	51	49
0.2	0.1667	48	53	52	54	44
0.22	0.1803	43	47	45	43	38
0.24	0.1935	47	44	42	47	40
0.26	0.2063	46	43	39	44	46
0.28	0.2188	45	44	38	39	45

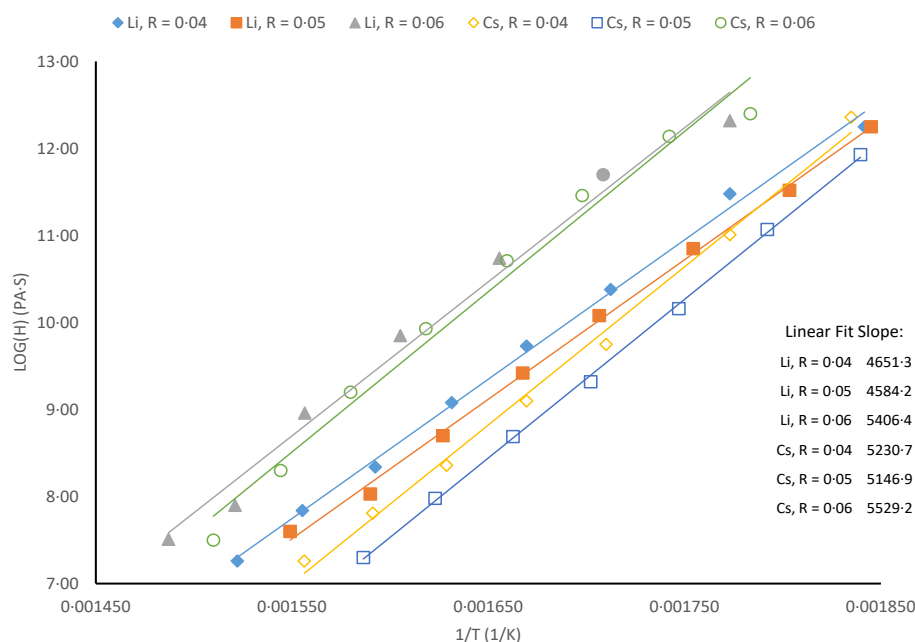


Figure 7. Viscosity data for lithium borate and caesium borate glasses. Compositions range from $R=0.04$ to 0.06 , where R is the molar ratio of alkali oxide to boron oxide. The inset table displays slopes of each composition assuming a linear response. Slopes are given in K^{-1} . The error in log viscosity is about 0.05 and is smaller than the symbol size [Colour available online]

glass are smaller than those of the lithium-modified glass, but the ΔT_g 's of the two glasses are similar.

The viscosities near the ΔT_g maxima are anomalous in that both systems exhibit minimal slope at $R=0.05$.

The fictive temperature (T_f) of these glasses is not single valued, but exhibits spatial fluctuations, which follow the fluctuations in both density and composition (for glasses with more than one component) that characterize the structure of any glass. For glasses having two or more components with different chemical natures, in this case a basic network modifier and an acidic network former, the compositional fluctuations can be explained in terms of the chemical groupings that characterize the structure of the glass, as predicted by thermodynamic modelling.⁽⁴⁾ We interpret and

extend these ideas to indicate that as the supercooled melt is quenched, the structure of different chemical groupings will become frozen in at different temperatures. This can be seen from the curved section of the $V-T$ plot for a glass former.⁽⁸⁾ We also suggest that the width of the glass transition thus corresponds to the range of T_f for the chemical groupings.

The problem then reduces to an estimation of the fictive temperatures for each of the chemical groupings in each species as a function of composition, which is related to their average connectivity, $\langle c \rangle$.⁽⁸⁾ The higher $\langle c \rangle$ is, the higher T_f is, although this is not a linear relationship. T_f will also vary according to the degree to which its network is constrained by its immediate neighbours. Finally, even at compositions associated with crystalline stoichiometries

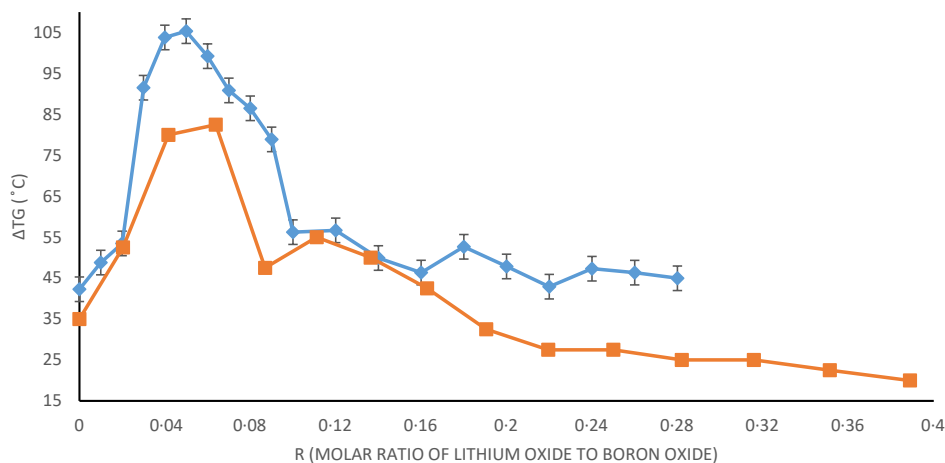


Figure 8. Present ΔT_g data from lithium borate glasses (blue) and those obtained by Kodama et al.⁽³⁾ (orange), both as a function of R (molar ratio of lithium oxide to boron oxide) [Colour available online]

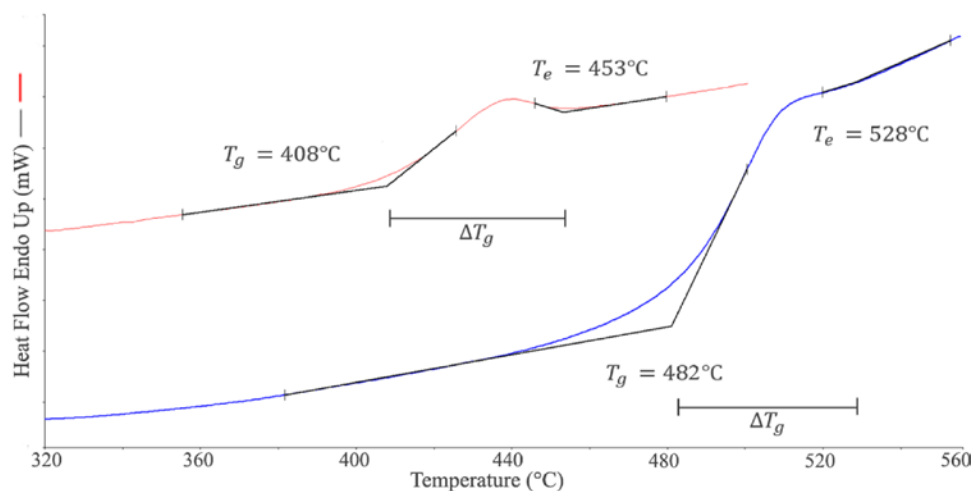


Figure 9. Superimposed DSC runs of $R=0.26$ lithium borate (bottom) and $R=0.28$ caesium borate (top). The two glasses exhibit transitions beginning and ending at different temperatures, but with similar ΔT_g values of 46 and 45°C, respectively [Colour available online]

(pentaborate, triborate, diborate, etc.), a glass has a range of chemical grouping species, not just those of the given stoichiometry. However, usually this stoichiometry predominates, as shown by the thermodynamic modelling of Vedishcheva,^(4,10) and so a rough guide as to the relative value of T_f for a given chemical grouping could be obtained by measuring T_g at the composition at which its contribution to the chemical structure is a maximum.

A possible interpretation of the present anomaly in the data from the alkali borate glasses is now possible. The lithium and caesium systems are the focus herein and it is noted that the chemical stoichiometries for any given system have similar compositions to those of the crystalline compounds. For the latter system, the chemical groupings that are likely to be present as a significant fraction over the studied compositional range are B_2O_3 (boroxol rings), caesium enneaborate, which consists of triborate and boroxol groups ($Cs_2O \cdot 9B_2O_3$), and caesium pentaborate, $Cs_2O \cdot 5B_2O_3$ or Cs_5B (in very small quantities).⁽¹¹⁾ Furthermore, no caesium tetraborate can be expected, particularly because the stoichiometry is $3Cs \cdot 13B$ rather than $5Cs \cdot 19B$.⁽⁹⁾ Thus for the caesium borate system, we have B_2O_3 ($\langle c \rangle = 3$; floppy), Cs_9B ($\langle c \rangle = 3.33$; floppy) and Cs_5B , in small quantities, ($\langle c \rangle = 4$; stressed-rigid).⁽⁶⁾ Spectroscopic evidence for the presence of these units has been found from neutron scattering and nuclear magnetic resonance.^(12,13) The situation for the Li–B system is different, in that both lithium enneaborate and pentaborate groups are essentially absent. Hence the only significant chemical groupings are B_2O_3 ($\langle c \rangle = 3$; floppy) and Li_3B (triborate units with $\langle c \rangle = 4$; stressed-rigid). Also, the triborate groups in caesium-modified glasses at low R are incorporated into floppy Cs_9B chemical groupings, whereas those in the lithium-modified glasses are present as stressed-rigid Li_3B groupings, see Figure 10. Looking at the variation of T_g with R , it is apparent

that T_g at the Cs_9B composition is lower than that at the Li_3B composition,⁽³⁾ and so the spread in T_g at R around the peak in ΔT_g in the lithium borate system will be much lower for the caesium system versus the lithium system.

Although the samples prepared for this paper as well as those of other researchers do not show visible signs of liquid–liquid immiscibility it is possible that this occurs at a sub-visible wavelength scale (less than 400 nm) depending on temperature and time employed. This result has been reported by Shaw & Uhlman.⁽¹⁴⁾ However, in all cases in this work there appeared only one glass transition event. This is true both for samples cooled slowly (about 0.7°C/s and quickly (greater than 10000°C/s). In addition, thermoscans run at differing heating rates all showed this anomaly at approximately the same magnitude. Furthermore, the compositional range for the liquid–liquid immiscibility reported by Shaw & Uhlmann (centred around $R=0.11$) does not match where the anomaly occurs (at $R=0.05$). Also, in their work, the caesium system showed more growth of phase separation than in the lithium system; were phase

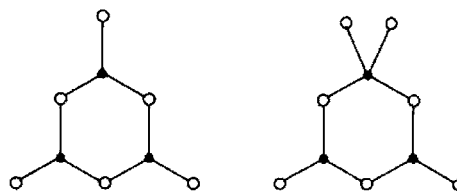


Figure 10. The boroxol and triborate structural groups (black filled dots are boron and open dots are oxygen). The number of connections per group are 3 and 4, respectively. The T_f of the triborate group is higher than that of the boroxol ring. The enneaborate group that appears in the caesium borate system is composed of two boroxol groups and one triborate group and has 3.3 connections per group and an intermediate T_f between the boroxol and triborate values

separation a cause, this would reverse the trends of the present results.

In 1977 Golubkuv *et al.*⁽¹⁵⁾ reported on the presence and growth of liquid–glass phase separation in the lithium borate system. This was seen near the composition ($R=0.05$) at which the T_g anomaly is being reported here. Their data may be related to the observations reported in the present paper.

5. Conclusions

A ΔT_g anomaly has been observed in alkali borate glasses. The glasses of all families have T_g values at similar temperatures in the critical range R ($0 \leq R \leq 0.10$). However, the transitions of the lithium-modified (and to a smaller extent sodium-modified) glasses are significantly wider than the transitions of glasses modified with potassium, rubidium, or caesium.

The ΔT_g anomaly may be explained in terms of the variation of the fictive temperature of the glasses due to structural grouping variations as given in the thermodynamic modelling of chemical species as proposed by Vedishcheva *et al.*⁽⁴⁾ The ideas of constraint theory have been employed as well. The lithium and caesium borate systems are composed of different superstructural groups leading to a wider distribution of fictive temperatures in the lithium borate system compared with caesium. This may be the source of the anomaly reported here.

Acknowledgements

The authors wish to acknowledge Adrian Wright, Natalia Vedischeva, Collin Wilkinson, Evgeny Pakhomenko, and Wesley Miller. Also, financial support of the National Science Foundation under grant

DMR 1407404 for funding this research. Coe College is thanked for providing further assistance.

References

1. Munhollon, T. Private Communication.
2. Starkenburg, D. & Perez, B. Private Communication.
3. Kodama, M., Kojima, S., Feller, S. & Affatigato, M. Borate anomaly, anharmonicity and fragility in lithium borate glasses. *Phys. Chem. Glasses*, 2005, **46** (2), 190–193.
4. Vedishcheva, N. M. & Wright, A. C. Chemical structure of oxide glasses: a concept for establishing structure–property relationships. In: *Glass. Selected properties and crystallization*, Ed. J. W. P. Schmelzer, De Gruyter, Berlin/Boston, 2014, Chapter 5, p. 269–299.
5. Wright, A. C. Borate structures: crystalline and vitreous. *Phys. Chem. Glasses: Eur. J. Glass Sci. Technol. B*, 2010, **51**, 1–39, and unpublished calculations of N. M. Vedishcheva.
6. Mauro, J. C., Gupta, P. K. & Loucks, R. J. Composition Dependence of Glass Transition Temperature and Fragility. II. A Topological Model of Alkali Borate Liquids. *J. Chem. Phys.*, 2009, **130**, 234503–1–234503–8.
7. Zanutto, E. D. *Cerâmica*, 1983, **29** (162), 135–139. Zanutto, E. D. PhD Thesis, Sheffield University, 1982, pp. 44–50.
8. This is a Zirconia-Alumina-Silica refractory material developed in EDZ's lab. Its microstructure contains mullite-ZrO₂ and a small amount of residual glass phase.
9. We do not have the Poisson ratios for all these borate glasses, so 0.5 was used as an approximate value in the calculations. This is justified as we were looking just at viscosity trends of closely spaced compositions (3–7% alkali oxide).
10. Wright, A. C. Crystalline-like ordering in melt-quenched network glasses? *J. Non-Cryst. Solids*, 2014, **401**, 4–26.
11. Vedishcheva, N. M. Unpublished data.
12. Faaborg, M., Goranson, K., Barnes, N., Trondle, E., Rice, R., Chace, M., Montgomery, L., Koehler, A., Lindeberg, Z., Holland, D., Smith, M., Affatigato, M., Singleton, S. & Feller, S. A ¹⁰B NMR Study of Trigonal and Tetrahedral Borons in Ring Structured Borate Glasses and Crystals. *Phys. Chem. Glasses: Eur. J. Glass Sci. Technol. B*, 2015, **56** (5), 177.
13. Sinclair, R. N., Haworth, R., Wright, A. C., Taylor, J. W., Vedischeva, N. M., Polyakova, I. G., Shakhmatkin, B. A., Feller, S. A., Affatigato, M., Winslow, D., Rijal, B. & Edwards, T. Neutron Spectroscopic Studies of Caesium Borate Crystals and Glasses. *Phys. Chem. Glasses: Eur. J. Glass Sci. Technol.*, 2006, **47** (4), 405–411.
14. Shaw, R. R. & Uhlmann, D. R. Subliquidus Immiscibility in Binary Alkali Borates. *J. Am. Ceram. Soc.*, 1968, **51** (7), 377–382.
15. Golubkuv, V. V., Titov, A. P., Vasleski, T. N. & Porai-Koshits, E. A. Phase Separation in Alkali Borate Glasses. *Fiz. Khim. Stekla*, 1977, **3** (4), 306–311.